Arctic organic aerosol measurements show particles from mixed combustion in spring haze and from frost flowers in winter

P. M. Shaw,[1] L. M. Russell,[1] A. Jefferson,[2] and P. K. Quinn[3]

[1] Submicron atmospheric aerosol particles were collected between 1 March 2008 and 1 March 2009 at Barrow, Alaska, to characterize the organic mass (OM) in the Arctic aerosol. Organic functional group concentrations and trace metals were measured with FTIR on submicron particles collected on Teflon filters. The OM varied from 0.07 μg m^{-3} in summer to 0.43 μg m^{-3} in winter, and 0.35 μg m^{-3} in spring, showing a transition in OM composition between spring and winter. Most of the OM in spring could be attributed to anthropogenic sources, consisting primarily of alkane and carboxylic acid functional groups and correlated to elemental tracers of industrial pollution, biomass burning, and shipping emissions. PMF analysis associated OM with two factors, a Mixed Combustion factor (MCF) and an Ocean-derived factor (ODF). Back trajectory analysis revealed that the highest fractions of the MCF were associated with air masses that had originated from northeastern Asia and the shipping lanes south of the Bering Straits. The ODF consisted of organic hydroxyl groups and correlated with organic and inorganic seawater components. The ODF accounted for more than 55% of OM in winter when the sampled air masses originated along the coastal and lake regions of the Northwest Territories of Canada. Frost flowers with organic-salt coatings that arise by brine rejection during sea ice formation may account for this large source of carbohydrate-like OM during the ice-covered winter season. While the anthropogenic sources contributed more than 0.3 μg m^{-3} of the springtime haze OM, ocean-derived particles provided comparable OM sources in winter. **Citation:** Shaw, P. M., L. M. Russell, A. Jefferson, and P. K. Quinn (2010), Arctic organic aerosol measurements show particles from mixed combustion in spring haze and from frost flowers in winter, *Geophys. Res. Lett.*, *37*, L10803, doi:10.1029/2010GL042831.

1. Introduction

[2] Changing snow and sea ice cover, associated albedo feedbacks and large seasonal variation in incoming sunlight make the Arctic region especially sensitive to recent climate change [*Garrett et al.*, 2009]. *Li and Winchester* [1990] proposed organic carbon was a significant fraction of the total submicron aerosol mass that they measured at Barrow, and subsequent studies showed this fraction could account for 20–30% of the submicron aerosol mass concentration [*Li and Winchester*, 1993]. *Quinn et al.* [2002] measured three years of ionic species at Barrow and attributed much of the residual in the submicron mass balance to the organic components. Transported Arctic aerosol particles could result in either positive or negative feedbacks to global warming [*Tomasi et al.*, 2007], making understanding the role of organics in the Arctic atmosphere crucial for quantifying the direct and indirect aerosol effects in this sensitive region.

[3] Long term observations of seasonal patterns in organic carbon concentration and speciation were reported by *Kawamura et al.* [1996] for Alert, Canada, and *Ricard et al.* [2002] in Sevettijarvi, Finland. In this work, we report the first year-long study of organic mass (OM) functional group composition in submicron particles in the Arctic region. The measurements were performed at the National Oceanic and Atmospheric Administration (NOAA) Earth System Research Laboratory (ESRL) site at Barrow, collocated with ongoing measurements of inorganic ions, optical, and physical metrics of aerosol particles and other atmospheric characteristics. We show that the submicron organic functional group composition provides important insight on the sources and composition of both the well known springtime Arctic haze and the substantial OM contributions from frost flower particles in wintertime organic mass concentrations.

2. Methods

[4] Beginning in March 2008, automated measurements were maintained by NOAA ESRL staff at their laboratory in Barrow, Alaska, using an 8-sample rotating filter holder (described by *Quinn et al.* [2002]) modified to replace materials that outgas volatile organic compounds with metal or Delrin components. The filter holder exposes 8 different 47 mm diameter Teflon filters to ambient air pulled through a warmed inlet at 30 L min^{-1}. Filters were exposed for 24-hr in winter and spring and 96-hr in summer when aerosol concentrations are low. Filters were sealed and frozen during transport and storage. To avoid contamination from the town of Barrow, sector control was used to collect samples only when wind speed was above 0.5 m s^{-1} and direction was between 0° and 130° (60% of sampling time). Fourier transform infrared (FTIR) spectra were collected for each filter in a temperature and humidity controlled clean room to measure the absorption of organic functional groups and convert to mass [*Maria et al.*, 2002; *Gilardoni et al.*, 2007] using an automated algorithm [*Russell et al.*, 2009]. We quantified saturated aliphatic CCH (alkane group), carboxylic COH with associated C=O in an acid group COOH, non-

[1]Scripps Institution of Oceanography, University of California, San Diego, La Jolla, California, USA.
[2]Cooperative Institute for Research in Environmental Science, University of Colorado at Boulder, Boulder, Colorado, USA.
[3]Pacific Marine Environmental Laboratory, NOAA, Seattle, Washington, USA.
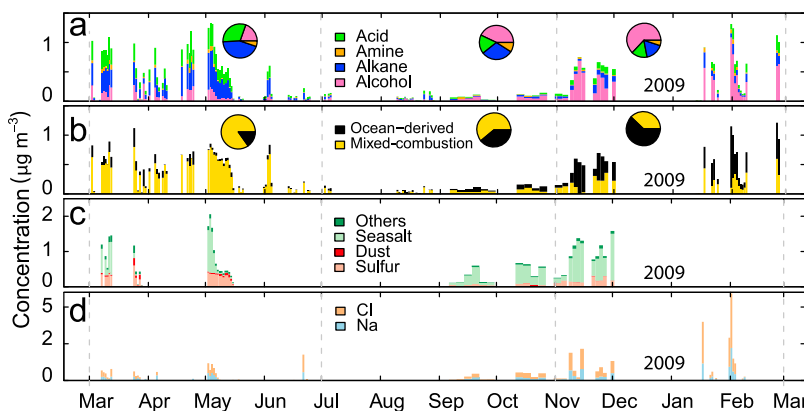
Figure 1. Time series of measured atmospheric aerosol component concentrations. (a) FTIR organic functional groups; (b) PMF factors; (c) XRF trace metals; (d) IC sea salt. Bar widths correspond to durations of collected filters. Inset pies indicate time weighted seasonal averages.

acidic hydroxyl COH (alcohol group), and primary amine CNH_2 groups [*Russell et al.*, 2009]. Non-acidic carbonyl C=O, aromatic and unsaturated aliphatic (alkene) functional groups are omitted because they were below detection for the majority of the study. Of the 118 filters collected, 47 were sent to Chester laboratories for X-ray fluorescence (XRF) spectroscopy [*Maria et al.*, 2002] to quantify S, Na, Cl, Si, Al, Fe, Ti, Ca, Mg, K, V, Zn, and Br (additional measured elements were below detection for a majority of samples). Ion chromatography was used to quantify ionic composition of 66 filters [*Quinn et al.*, 2002].
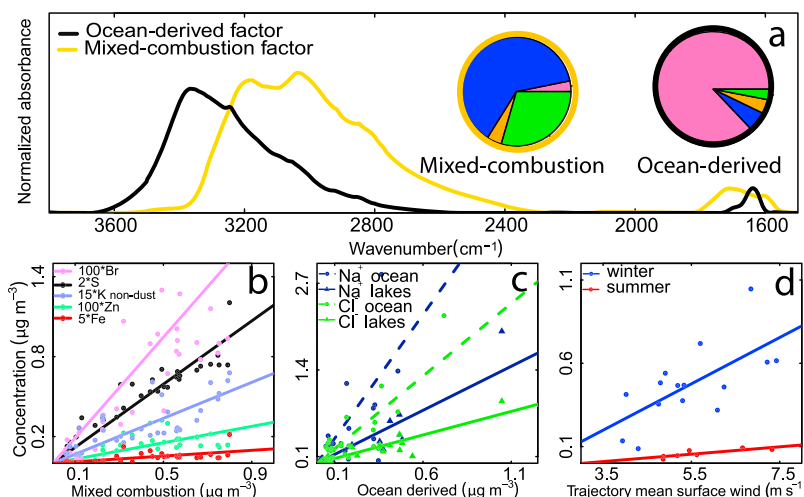
3. Results

[5] OM concentrations varied significantly from March 2008 to March 2009, as shown in Figure 1. Based on OM concentration and functional group composition, we have separated the measurements into three seasons, which are summarized in Figure 1: spring (March to June), summer (July to October), and winter (November to February). These seasons were determined according to the following criteria: (1) spring months had daily-averaged OM concentrations higher than 1 μg m^{-3} and consisted of approximately half alkane groups with the other half split between carboxylic acid and alcohol groups; (2) summer months generally had 4-day averaged OM concentrations below 0.5 μg m^{-3} and consisted of about half alkane and half alcohol group fractions; (3) winter month filters generally had the highest OM concentrations and were primarily alcohol groups. A three-year aerosol study at Barrow by *Quinn et al.* [2002] used different cutoffs for 1997–2000 for the inorganic aerosol concentration and composition, with February omitted as transitional and October identified as winter. In any given year the characteristics of February and October are arguably transitional, but for OM October 2008 resembles the lower OM, concentrations and wind speeds of summer rather than those of winter (Figure 1a). Similarly February 2009 represented a continuation of the high organic hydroxyl composition of winter rather than the carboxylic acid fraction that characterized the rest of spring.

[6] Positive matrix factorization (PMF) provides a tool to apportion sources based on the repeated occurrence of similar spectral features during a series of ambient measurements in a single region [*Paatero and Tapper*, 1994].

PMF of FTIR spectra has been used to identify combinations of organic functional groups that combine linearly in time to reproduce the original observed OM time series [*Russell et al.*, 2009]. PMF was performed on the 118 spectra collected at Barrow. FPEAK rotation values of −0.2, 0, and 0.2 were tested for 2 through 6 factors resulting in negligible differences, so FPEAK = 0 is used here. We chose the 2-factor solution because solutions with 3 to 6 factors reproduced less than 98% of the original OM concentrations or included one or more non-independent (r > 0.3) or physically unrealistic spectra. The time series of the best 2-factor solution is shown in Figure 1b, with the associated spectra and organic functional group composition in Figure 2a. The first PMF factor (defined as Mixed Combustion MCF) accounts for much of the carboxylic acid and alkane group concentrations, and the second factor (defined as Ocean-derived, ODF) accounts for most of the organic hydroxyl group concentrations.

[7] Correlations of tracers with the two resulting PMF factor OM concentrations are summarized in Figure 2b for XRF metals and Figure 2c for IC sea salt ions, which were used to identify the possible sources associated with each OM factor. We describe correlations as strong for r > 0.75 and mild for 0.5 < r < 0.75. The first PMF factor is correlated strongly to S and non-dust K and mildly to V. Since V is a tracer for oil combustion (including from shipping) and non-dust K is a tracer for biomass burning, we refer to this factor as the MCF [*Cachier et al.*, 1995; *Gilardoni et al.*, 2009; *Isakson et al.*, 2001]. The alkane and carboxylic acid group contributions to the OM are characteristic of processed emissions from oil burning and have also been seen in biomass burning [*Russell et al.*, 2009]. The second factor correlates mildly for all IC measurements of Na$^+$ and Cl$^-$. We call this factor ODF based on this correlation to NaCl as well as the similarity of the spectrum of the second factor to other ocean-derived organic particles [*Russell et al.*, 2010].

[8] To provide an indication of the geographic location of the emissions, potential source contribution functions (PSCF) [*Pekney et al.*, 2006] were calculated from five-day HYSPLIT isentropic back trajectories [*Draxler and Rolph*, 2003] (Figures 3a–3f). The HYSPLIT model was run every four hours during each filter with a starting altitude of 500 m and points above 1000 m omitted. The PSCF map for the

Figure 2. Results of two-factor PMF solution. (a) Baselined spectra. Colors for spectra correspond to those given in Figure 1b. Inset pies indicate the fractional functional group composition for each factor; (b) correlations of MCF and XRF trace metal concentrations (S: r = 0.96; non-dust K: r = 0.80; V: r = 0.61; Fe: r = 0.69; Zn: r = 0.69; Br: r = 0.68); (c) correlations of ODF and IC salt concentrations (overall Cl⁻: r = 0.63; Na⁺: r = 0.60), with separate lines for filters influenced by lakes (solid lines; Cl⁻: r = 0.86; Na⁺: r = 0.77) and ocean-only (dashed lines; Cl⁻: r = 0.74; Na⁺: r = 0.81); (d) back trajectory-weighted mean wind speed versus ODF observations with fraction >0.5 for summer (red; [ODF] = 0.037*wind speed - 0.17; r = 0.87) and winter (blue; [ODF] = 0.24*wind speed - 0.84; r = 0.67).

MCF (Figures 3a, 3c, and 3e) shows potential source regions over Siberia (between 60–70° N and west of 180°), which correspond to locations of forest fires observations by MODIS during the observation period (Figure 3g). Commercial shipping traffic (Figure 3g) was estimated from the total March 2008 to March 2009 frequency of meteorological observations reported from ships [*Corbett et al.*, 1999] and were found to overlap the high MCF PSCF regions south of 60° N between 160° and −160°. These high MCF regions overlap industrial regions of northern Russia (surrounding Anadyr, Russia (Figure 3g)), where smelters, coal mining and other industry contribute significant anthropogenic particle emissions [*Arctic Monitoring and Assessment Programme*, 1998].

4. Discussion

[9] Long-range transported pollution from lower latitudes including black carbon, sulfates, soil dust, and biomass burning smoke have dramatic influences on what should otherwise be a clean Arctic environment [*Barrie and Barrie*, 1990]. Figures 1c and 1d show the concentrations of metals and salts measured during the study, including occasional dust species events (Al, Ti, and Si) and seasonal changes in sea salt (Na, Cl) and sulfur. Emissions from burning forests have been shown to produce non-acidic carbonyl groups in addition to carboxylic acid groups [*Russell et al.*, 2009]. This MCF also correlates with industrial trace metals (Fe, Zn, and Br), as shown in Figure 2b, indicating that urban areas such as Anadyr also contributed to the MCF.

[10] *Russell et al.* [2010] show that the alcohol functional group measured by FTIR is representative of carbohydrate-like compounds, including saccharides, associated with ocean-derived particles emitted by bubble bursting during wave breaking. The ODF at Barrow has very similar features in the FTIR spectrum (Figure 2a), including the broad organic hydroxyl absorbance between 3200 and 3500 cm⁻¹. Because

local wind speed may be a poor representation of sea salt emission in regions removed from the receptor, we averaged gridded 1° × 1° NCEP reanalysis surface winds along each five day back trajectory that passed through the boundary layer for each filter. The linear fit of trajectory weighted
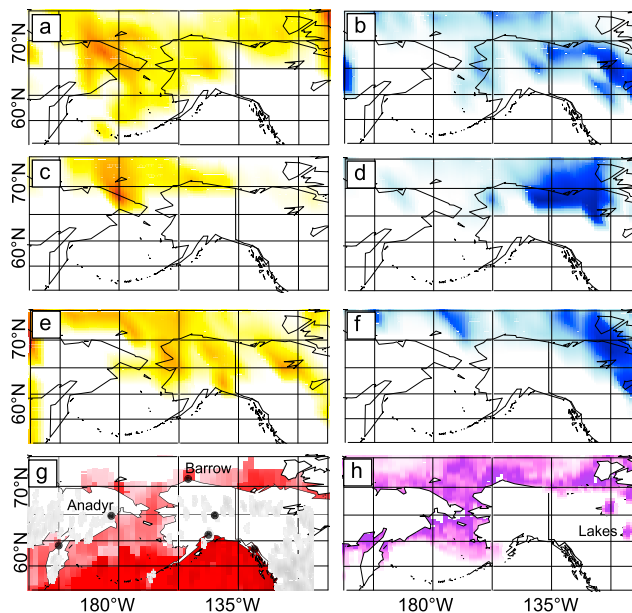
Figure 3. Density maps for observation period of 5-day PSCF for MCF (highest in dark orange) and ODF (highest in dark blue); (a, b) spring; (c, d) summer; (e, f) winter; (g) anthropogenic sources: cities with population >10000 (Anadyr, Russia; Barrow, Fairbanks, Anchorage and Juneau, Alaska); estimated shipping density from NCEP marine observations (highest in dark red); MODIS fire locations (greyscale); (h) modeled density of potential frost flower regions (highest in dark purple).

mean wind speed (Figure 2d) for summer ODF compares well with the observations of a similar marine factor versus wind speed in the Arctic during ice free conditions [*Russell et al.*, 2010]. The winter best fit line has a higher dependence of particle concentration on wind speed, which is likely associated with the higher particle production rate as a function of wind speed from frost flowers than from bubble bursting. There appears to be little OM at low wind speeds or those above 8 m s^{-1}, consistent with ranges found in other frost flower studies [*Obbard et al.*, 2009].

[11] The potential source region identified for the ODF (Figures 3b, 3d, and 3f) overlaps in summer with the ocean and in winter with sea-ice-land fringes and the Great Bear and Great Slave lakes (Figure 3h). The replacement of coastal waters by sea ice in winter, as well as the higher slope of the emitted ODF with average trajectory wind speed, support a different mechanism for the formation of ocean-derived organic particles in winter. These results suggest that surface frost flowers formed on the sea and lake ice provide the source of the ODF at Barrow in winter. Frost flowers grow as ice skeletons from supersaturated water vapor at the ice-air interface. Brine rejected to pools on the sea ice surface during ice formation from seawater provides a highly saline source that can be wicked up onto frost flowers [*Alvarez-Aviles et al.*, 2008] and likely includes sea water dissolved organic matter (DOM) [*Thomas and Dieckmann*, 2003; *Stein and MacDonald*, 2004; *Papadimitriou et al.*, 2007; *Giannelli et al.*, 2001; *Belzile et al.*, 2002].

[12] The high PSCF region for the ODF factor was east of Barrow amid the islands of the Northwest Territories of Canada and is also the location of young coastal ice rivers and lakes where frost flowers form [*Beaudon and Moore*, 2009]. To identify areas of potential frost flower (PFF) coverage, we used the 1-d algorithm for gridded NCEP reanalysis surface temperature and sea ice concentrations as described by *Kaleschke et al.* [2004]. High density PFF regions along the northern coast of Alaska and Canada and among the lakes of the Northwest Territories (Figure 3h) coincide with high density of back trajectories for the ODF PSCF regions. Separating the observations with trajectories that passed over the Great Bear and Great Slave lakes from those that passed only over ocean results in two separate correlations of ODF with Na$^+$ and Cl$^-$, with slopes of 0.2 and 0.8, within the range 0.1 to 1 observed for oceans [*Russell et al.*, 2010]. Typically lakes contain a factor of 10 lower NaCl than oceans [*Thurman*, 1985]. Higher ODF per NaCl in lakes is consistent with the lower expected salt content of lakes relative to ocean brine. The smaller difference in the particle composition of a factor of 4 (rather than 10) is easily attributable to the order of magnitude uncertainty in DOC concentrations in both lakes and ocean surface waters (0.002 g L^{-1} to 0.02 gL^{-1} [*Thurman*, 1985]).

5. Conclusion

[13] Twelve months of submicron particle measurements at Barrow, Alaska, show that organic components contribute significant quantities of particle mass. Overall OM concentrations range from less than 0.5 μg m^{-3} in summer to often more 2 μg m^{-3} in winter and spring. Functional group composition also changed by season: alkane and carboxylic acid functional groups dominated spring composition and organic hydroxyl groups dominated winter. High OM con-

centrations from Asian biomass burning, ship traffic, and other industrial activities produced Arctic haze in spring, low concentrations in summer occurred when removal by precipitation is most efficient, and large concentrations in winter were caused by ocean-derived OM that is released from frost flowers. Through PSCF of PMF-based OM factors, we identified the probable locations of the two types of source emissions: 1) mixed combustion from urban areas in Siberia and the shipping lanes of the North Pacific in springtime; and 2) ocean-derived particles released from bubble bursting in summer and possibly from sea ice and lake ice frost flowers in winter. Frost flowers provide a source of particles in the Arctic region during winter, which results in surprisingly large concentrations of Arctic OM comparable to those observed during the springtime haze.

References

Alvarez-Aviles, L., W. R. Simpson, T. A. Douglas, M. Sturm, D. Perovich, and F. Domine (2008), Frost flower chemical composition during growth and its implications for aerosol production and bromine activation, *J. Geophys. Res.*, *113*, D21304, doi:10.1029/2008JD010277.

Arctic Monitoring and Assessment Programme (1998), Assessment report: Arctic pollution issues, 859 pp., Oslo.

Barrie, L., and M. Barrie (1990), Chemical components of lower tropospheric aerosols in the high Arctic: Six years of observations, *J. Atmos. Chem.*, *11*(3), 211–226.

Beaudon, E., and J. Moore (2009), Frost flower chemical signature in winter snow on Vestfonna ice cap, Nordaustlandet, Svalbard, *Cryosphere*, *3*, 147–154.

Belzile, C., J. Gibson, and W. Vincent (2002), Colored dissolved organic matter and dissolved organic carbon exclusion from lake ice: Implications for irradiance transmission and carbon cycling, *Limnol. Oceanogr.*, *47*(5), 1283–1293.

Cachier, H., C. Liousse, P. Buat-Menard, and A. Gaudichet (1995), Particulate content of savanna fire emissions, *J. Atmos. Chem.*, *22*(1), 123–148.

Corbett, J. J., P. S. Fischbeck, and S. N. Pandis (1999), Global nitrogen and sulfur inventories for oceangoing ships, *J. Geophys. Res.*, *104*(D3), 3457–3470, doi:10.1029/1998JD100040.

Draxler, R., and G. Rolph (2003), HYSPLIT (HYbrid Single-Particle Lagrangian Integrated Trajectory), Air Resour. Lab., NOAA, Silver Spring, Md. (Available at http://www.arl. noaa. gov/ready/hysplit4.html)

Garrett, T. J., M. M. Maestas, S. K. Krueger, and C. T. Schmidt (2009), Acceleration by aerosol of a radiative-thermodynamic cloud feedback influencing Arctic surface warming, *Geophys. Res. Lett.*, *36*, L19804, doi:10.1029/2009GL040195.

Giannelli, V., D. Thomas, C. Haas, G. Kattner, H. Kennedy, and G. Dieckmann (2001), Behaviour of dissolved organic matter and inorganic nutrients during experimental sea-ice formation, *Ann. Glaciol.*, *33*(1), 317–321.

Gilardoni, S., et al. (2007), Regional variation of organic functional groups in aerosol particles on four U.S. east coast platforms during the International Consortium for Atmospheric Research on Transport and Transformation 2004 campaign, *J. Geophys. Res.*, *112*, D10S27, doi:10.1029/2006JD007737.

Gilardoni, S., et al. (2009), Characterization of organic ambient aerosol during MIRAGE 2006 on three platforms, *Atmos. Chem. Phys*, *9*, 5417–5432.

Isakson, J., T. Persson, and E. Selin Lindgren (2001), Identification and assessment of ship emissions and their effects in the harbour of Goteborg, Sweden, *Atmos. Environ.*, *35*(21), 3659–3666.

Kaleschke, L., et al. (2004), Frost flowers on sea ice as a source of sea salt and their influence on tropospheric halogen chemistry, *Geophys. Res. Lett.*, *31*, L16114, doi:10.1029/2004GL020655.

Kawamura, K., H. Kasukabe, and L. A. Barrie (1996), Source and reaction pathways of dicarboxylic acids, ketoacids and dicarbonyls in arctic aerosols: One year of observations, *Atmos. Environ.*, *30*(10–11), 1709–1722.

Li, S.-M., and J. Winchester (1990), Haze and other aerosol components in late winter Arctic Alaska, 1986, *J. Geophys. Res.*, *95*(D2), 1797–1810.

Li, S., and J. W. Winchester (1993), Water soluble organic constituents in Arctic aerosols and snow pack, *Geophys. Res. Lett.*, *20*(1), 45–48, doi:10.1029/92GL02918.

Maria, S., L. Russell, B. Turpin, and R. Porcja (2002), FTIR measurements of functional groups and organic mass in aerosol samples over the Caribbean, *Atmos. Environ.*, *36*(33), 5185–5196.

Obbard, R. W., H. K. Roscoe, E. W. Wolff, and H. M. Atkinson (2009), Frost flower surface area and chemistry as a function of salinity and temperature, *J. Geophys. Res.*, *114*, D20305, doi:10.1029/2009JD012481.

Paatero, P., and U. Tapper (1994), Positive matrix factorization: A nonnegative factor model with optimal utilization of error estimates of data values, *Environmetrics*, *5*(2), 111–126.

Papadimitriou, S., D. Thomas, H. Kennedy, C. Haas, H. Kuosa, A. Krell, and G. Dieckmann (2007), Biogeochemical composition of natural sea ice brines from the Weddell Sea during early austral summer, *Limnol. Oceanogr.*, *52*(5), 1809–1823.

Pekney, N., C. Davidson, L. Zhou, and P. Hopke (2006), Application of PSCF and CPF to PMF-modeled sources of PM 2.5 in Pittsburgh, *Aerosol Sci. Technol.*, *40*(10), 952–961.

Quinn, P. K., T. L. Miller, T. S. Bates, J. A. Ogren, E. Andrews, and G. E. Shaw (2002), A 3-year record of simultaneously measured aerosol chemical and optical properties at Barrow, Alaska, *J. Geophys. Res.*, *107*(D11), 4130, doi:10.1029/2001JD001248.

Ricard, V., J.-L. Jaffrezo, V.-M. Kerminen, R. E. Hillamo, M. Sillanpaa, S. Ruellan, C. Liousse, and H. Cachier (2002), Two years of continuous aerosol measurements in northern Finland, *J. Geophys. Res.*, *107*(D11), 4129, doi:10.1029/2001JD000952.

Russell, L. M., S. Takahama, S. Liu, L. N. Hawkins, D. S. Covert, P. K. Quinn, and T. S. Bates (2009), Oxygenated fraction and mass of organic aerosol from direct emission and atmospheric processing measured on the R/V Ronald Brown during TEXAQS/GoMACCS 2006, *J. Geophys. Res.*, *114*, D00F05, doi:10.1029/2008JD011275.

Russell, L., L. Hawkins, A. Frossard, P. Quinn, and T. Bates (2010), Carbohydrate-like composition of submicron atmospheric particles and their production from ocean bubble bursting, *Proc. Natl. Acad. Sci. U. S. A.*, doi:10.1073/pnas.090890517, in press.

Stein, R., and R. W. MacDonald (Eds.) (2004), *The Organic Carbon Cycle in the Arctic Ocean*, Springer, Berlin.

Thomas, D. N., and G. S. Dieckmann (Eds.) (2003), *Sea Ice: An Introduction to Its Physics, Chemistry, Biology and Geology*, Blackwell Sci., Oxford, U. K.

Thurman, E. (1985), *Organic Geochemistry of Natural Waters*, Kluwer Acad., Dordrecht, Netherlands.

Tomasi, C., et al. (2007), Aerosols in polar regions: A historical overview based on optical depth and in situ observations, *J. Geophys. Res.*, *112*, D16205, doi:10.1029/2007JD008432.

A. Jefferson, Cooperative Institute for Research in Environmental Science, University of Colorado at Boulder, 325 Broadway, Boulder, CO 80305, USA.

P. K. Quinn, Pacific Marine Environmental Laboratory, NOAA, 7600 Sand Point Way, NE, Seattle, WA 98115, USA.

L. M. Russell and P. M. Shaw, Scripps Institution of Oceanography, University of California, San Diego, Mail Code 0221, 9500 Gilman Dr., La Jolla, CA 92093, USA. (lmrussell@ucsd.edu)